

Mean-field approach to Pb-mediated growth of Ge on Si(111): Comparison with experiment and kinetic Monte Carlo simulations

Janusz Bęben,^{1,*} Czesław Oleksy,² Ivo Klik,³ and Tien T. Tsong⁴

¹*Institute of Experimental Physics, Wrocław University, Wrocław, Poland*

²*Institute of Theoretical Physics, Wrocław University, Wrocław, Poland*

³*Department of Physics, National Taiwan University, Taipei, Taiwan Republic of China*

⁴*Institute of Physics, Academia Sinica, Nankang, Taipei, Taiwan Republic of China*

(Received 9 August 2006; revised manuscript received 12 November 2006; published 9 January 2007)

Using a mean-field approximation we describe the early stages of growth of Ge on Si(111) mediated by a Pb surfactant. A set of rate equations is constructed for the time evolution of the number of clusters of a given size. The Ge atoms are deposited onto the surface at a constant flux rate, giving rise to a monomer population. The rates of growth and dissociation of the clusters are then calculated assuming that the dissociation energy $E_{diss} = [\bar{n}(s) - \lambda]E_{br} + E_d$, where E_{br} is the energy required to break one bond, and E_d is the diffusion energy of an isolated atom. Finally, $\bar{n}(s)$ is the average number of bonds broken when a cluster reduces its size s by 1. This dependence is obtained from a separate kinetic Monte Carlo experiment. The phenomenological constant $\lambda = 1.2$ by assumption. Our mean-field approximation describes the essential experimental results observed in Ge/Pb/Si(111) growth.

DOI: 10.1103/PhysRevB.75.045410

PACS number(s): 68.55.-a, 61.43.Hv, 02.70.Uu

I. INTRODUCTION

The use of surfactants in promoting the growth of smooth layers has attracted considerable attention of manufactures of advanced materials.^{1–12} Semiconductor substrates in particular have been extensively studied by surfactant-mediated epitaxy (SME).

An early stage of Ge growth on Si(111) with Pb as a surfactant was characterized by Hwang, Chang, and Tsong^{13–15} using a scanning tunneling microscopy technique. They observed the nucleation and growth of islands at varying experimental parameters like temperature, final concentration, or deposition flux. A phenomenological model explaining the observed growth features was recently proposed,¹⁶ and analyzed using kinetic Monte Carlo (KMC) technique.^{17,18} The main assumptions of the model¹⁶ are the following: (i) Ge atoms are deposited onto an Si(111) surface under a constant flux until the final concentration is reached, (ii) the deposited atoms diffuse on top of the surfactant, nucleate, and form clusters. (iii) a cluster of atoms can exchange position with the surfactants atoms and “dive” (We use the expression “cluster” for a Ge aggregate above the surfactant, while “island” refers to Ge atoms below the surfactant.) (iv) a cluster can grow or dissociate, (v) the exchange process between the Ge and Pb atoms (“diving”) is thermally activated and collective diving is energetically favorable, (vi) after the dive a cluster creates an island seed which can grow on account of incoming monomers, (vii) atoms below the surfactant cannot move, and a reverse event to the dive is forbidden.

In this paper we analyze this model using a mean-field approximation rather than the KMC technique used in our previous work.¹⁶

II. MEAN-FIELD MODEL

A key feature of the model is the interaction between Ge atoms which diffuse on top of the surfactant. We assume the

following energy barrier for the dissociation of a Ge atom from a cluster:

$$E_{diss} = [\bar{n}(s) - \lambda]E_{br} + E_d, \quad (1)$$

where $\bar{n}(s)$ is the average number of bonds broken when a cluster reduces its size s by 1, E_{br} is the energy required to break one bond, E_d is the energy barrier for the diffusion of an isolated Ge atom, and $\lambda = 1.2$ is a phenomenological constant to be discussed later.

According to Eq. (1) the dissociation barrier for an atom with a single bond to a cluster is lower than the barrier for diffusion of an isolated atom. Equivalently, we may say that atoms with one bond are repelled from the cluster while those with a larger number of bonds are attracted. As a result the clusters tend to be compact. Repulsive interactions were observed experimentally for some metal and Si atoms on metal surfaces by Tsong and Casanova.¹⁹ An edge atom of a cluster can change its position and in doing so it can reduce or increase the number of its bonds before dissociation. This is why within the mean-field approximation it is necessary to introduce an average number of bonds $\bar{n}(s)$ broken during the size reduction process.

Keeping in mind the interaction energy defined by Eq. (1) we now construct a set of rate equations for the variation in the number of clusters and islands of size s :

$$\begin{aligned} \frac{dn_1}{dt} &= F - 2D_1n_1n_1 - \sum_{s=2}^L D_1n_1n_s \\ &\quad + 2D_2n_2 + \sum_{s=3}^K D_n n_s, \end{aligned} \quad (2)$$

...

$$\frac{dn_s}{dt} = -D_1n_1n_s - D_s n_s + D_1n_1n_{s-1} + D_{s+1}n_{s+1},$$

$$\text{for } 1 < s \leq K, \quad (3)$$

$$\dots$$

$$\frac{dn_s}{dt} = -D_1 n_1 n_s + D_1 n_1 n_{s-1},$$

$$\text{for } K < s < L, \quad (4)$$

where D_1 is the rate of diffusion of an isolated Ge atom, D_s is the rate for dissociation of a single atom from a cluster of size s , and F is the deposition flux rate. Clusters with $1 < s \leq K$ find themselves on top of the surfactant, whereas clusters with $K < s < L$ have already dived.

Equation (2) describes the changes in the number of monomers. The individual terms have the following interpretation: The first term corresponds to an increase in the monomer number due to the flux F , the second term describes the decrease in the monomer number due to the creation of dimers, the third term represents the growth of clusters or islands of any size $s > 1$, the fourth term represents the dissociation of dimers, and the finally last term describes the dissociation of clusters of size $s > 2$.

The components of Eq. (3) mean, respectively, that the number of clusters of size s decreases if clusters of size s grow or dissociate (the first two terms), and increases if clusters of size $s-1$ grow or clusters of size $s+1$ dissociate (the last two terms).

In Eq. (4) the components which describe dissociation are missing. These equations describe the growth of islands which already are under the surfactant. The number of islands of size s decreases if islands of size s grow and increases if islands of size $s-1$ grow.

In our calculation the value L is set so high that all islands are actually smaller than L . We also set $K \equiv 7$ in the island density calculations to fulfill the assumption of a model of collective diving.

We use Eq. (1) to calculate the rates D_i with the function $\bar{n}(s)$ deduced from MC results. There is

$$D_1 = D_0 \exp\left[-\frac{E_d}{kT}\right], \quad (5)$$

$$D_2 = D_1 \exp\left[-\frac{[1-\lambda]E_{br}}{kT}\right], \quad (6)$$

and for $i > 2$

$$D_s = D_1 \exp\left[-\frac{[\bar{n}(s)-\lambda]E_{br}}{kT}\right]. \quad (7)$$

Here T is the temperature, k is the Boltzmann constant, $D_0 = 10^{11}/s$, and the deposition flux rate $F = 0.2 \text{ BL/min}$ (BL stands for bilayer). There is, further, $E_{br} = 0.4 \text{ eV}$, $E_d = 0.65 \text{ eV}$, and $\lambda = 1.2$. These numerical values have previously been used in our KMC simulations.^{16,17} The following sequence of inequalities results from the above assumptions:

$$D_2 > D_1 > D_3 > \dots > D_K > \dots > D_L. \quad (8)$$

We have chosen $\lambda > 1$ and the dimer dissociation rate D_2 is consequently the highest.

To get the required $\bar{n}(s)$ dependence we carried out a simple KMC experiment with rates R_n which depend on the

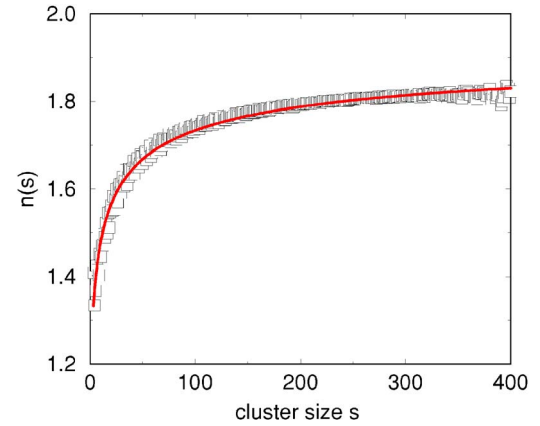


FIG. 1. (Color online) Average number of bonds $\bar{n}(s)$ broken when a cluster reduces its size s by one. The open squares are KMC results, and the solid line is the fitted curve discussed in text.

number of breaking bonds¹⁶ n : $R_n = D_1 \exp[(n-\lambda)E_{br}/kT]$ for $n = 1, \dots, 5$. Atoms initially placed randomly on a triangular lattice move and form clusters. To get $\bar{n}(s)$ for compact clusters of size s we simply set the duration of the cluster growth to be sufficiently long (a hundred hours). The typical dependence of an average number of broken bonds is shown in Fig. 1. The open squares are the KMC data while the solid line is the fitted curve given by the equation $\bar{n}(s) = 2 - 5.7 / (\sqrt{2.4s + 5.7})$. This formula is used in the mean-field calculations.

In general the function $\bar{n}(s)$ depends only weakly on temperature in the temperature range of our calculations, i.e., at 300–340 K. We neglect this dependence. Due to numerical problems it was not possible to broaden the temperature range.

We have solved the system of differential equations (2)–(4) using the fourth-order Runge-Kutta method.²⁰ The time step of the numerical integration has been chosen so as to provide a stable solution. The time step was reduced at elevated temperatures. However, the applicability of this method is limited to temperatures below 350 K, since otherwise the large number of equations needed to describe the process of island growth renders the computation prohibitively time consuming.

III. RESULTS

A. Island density

Hwang, Chang, and Tsong^{13–15} found in their STM experiments that there is a threshold coverage below which no islands grow. Close to this threshold the islands are large and have a fractal structure. For comparison we present in Figs. 2(a) and 2(b) both experimental and KMC results.¹⁶ Finally, Fig. 2(c) shows results obtained in the mean-field approximation. The shown threshold value of about 0.1 is obtained for $\lambda = 1.2$, and we find that a larger λ yields a larger threshold value. We can, of course, say nothing about the structure of clusters or islands from the mean-field approximation results.

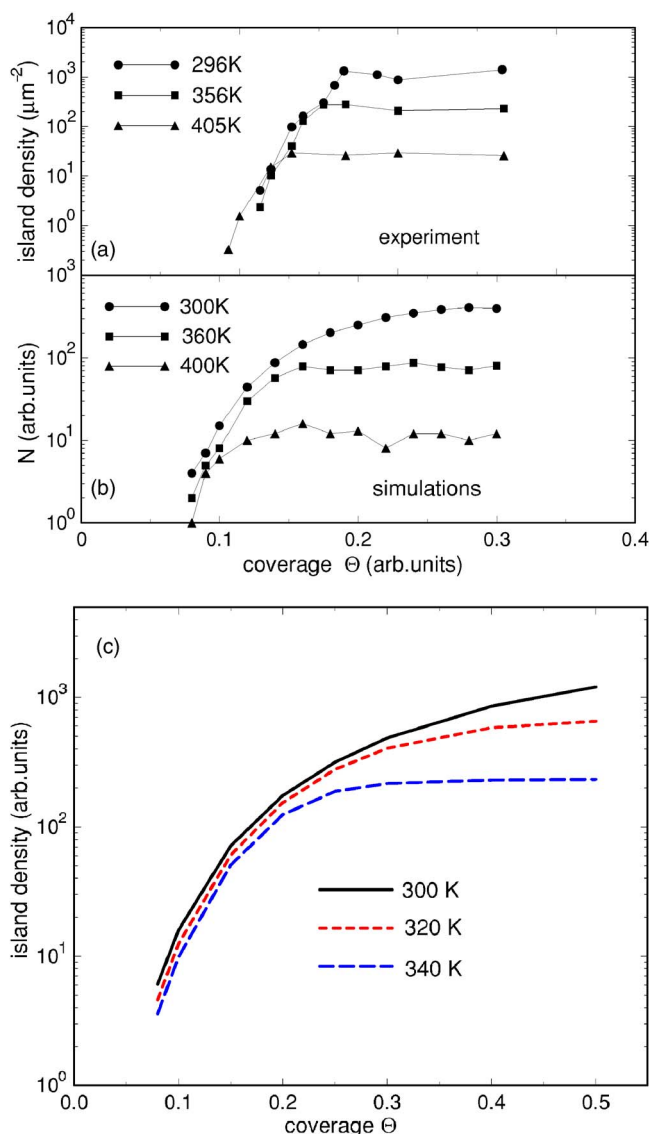


FIG. 2. (Color online) Island density vs coverage θ at different temperatures. Results: (a) experimental (Ref. 13), (b) KMC (Ref. 16), (c) mean-field approximation for $K=7$.

B. Time evolution

Two processes compete on the surfactant surface: cluster growth and cluster dissociation. A cluster which is in equilibrium with the surrounding monomers is called critical. Its size does not change in time. Smaller clusters tend to dissociate and larger clusters tend to grow. The size of the critical cluster decreases with increasing monomer concentration. The idea of the critical cluster can be applied to atoms above the surfactant only, because islands below the surfactant cannot dissociate. On top of the surfactant the clusters grow until they reach the size required for diving. The threshold effect occurs if the size of the critical cluster is larger than the dive size.

We do not have experimental data for the time evolution of Pb mediated growth of Ge films on Si(111). The experimental study is here rather difficult. However, we have studied the process in our previous work^{16,17} using the KMC

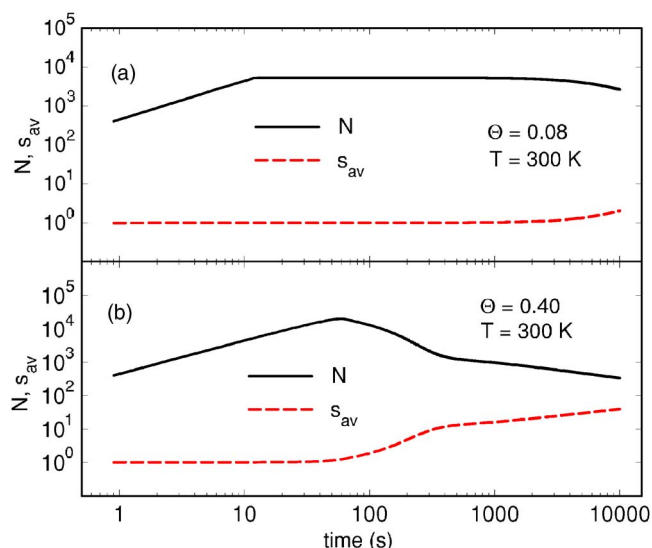


FIG. 3. (Color online) Mean-field results of the time evolution of the number of monomers N (solid lines) and the average cluster size s_{av} (dashed lines). The upper diagram (a) and lower diagram (b) show the time dependence at coverages below and above the threshold, respectively.

technique, and now we present the corresponding result obtained using the mean-field approach. To probe in detail the evolution on top of the surfactant we set K large enough to avoid diving.

Figure 3 shows the time evolution of the number of monomers and the average cluster size (s_{av}) for two final coverages that are chosen to be close (a) and far away (b) from the threshold value. In both plots the number of monomers N increases initially linearly due to deposition. After the initial stage both N and s_{av} remain almost constant for a long time, and then s_{av} increases and N decreases [Fig. 3(a)]. This effect is due to the fact that in our calculation the number of atoms is not necessarily an integer, while in experiment and in KMC the number of islands takes on only inte-

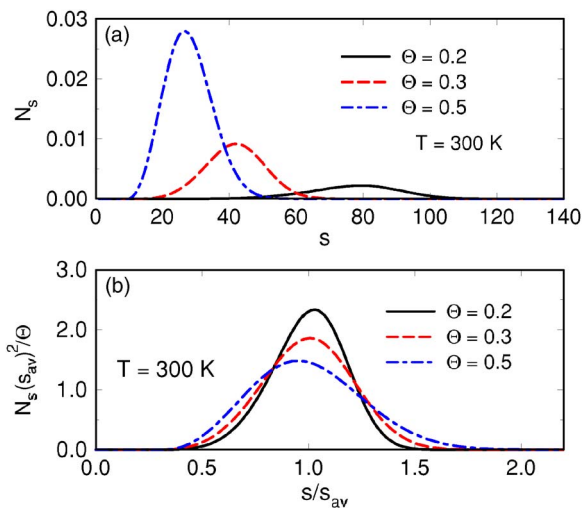


FIG. 4. (Color online) Scaling procedure for island size distributions at different concentrations θ . The diagrams (a) and (b) show nonscaled and scaled distributions, respectively.

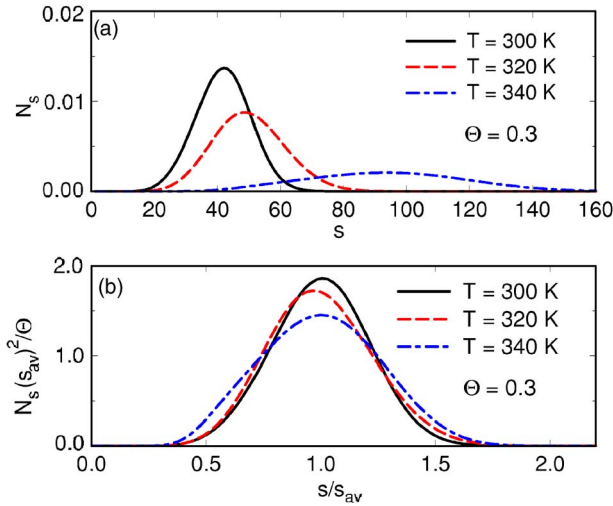


FIG. 5. (Color online) Scaling procedure for island size distributions at different growth temperatures. The diagrams (a) and (b) show nonscaled and scaled distributions, respectively.

ger values. Far away from the threshold [Fig. 3(b)], however, the average cluster size s_{av} starts to grow while the deposition is more or less finished. For times larger than 500 s the curves N and s_{av} both exhibit a power-law time dependence. This dependence indicates that Oswald ripening occurs in this time range.²¹ The size of the critical cluster increases here with time, and large clusters grow on account of dissociation of smaller ones. This effect was observed in KMC approach as well.¹⁷

C. Scaling

It was found both experimentally, and also in KMC simulations,¹⁷ that the growth of Ge/Pb/Si(111) obeys a scaling law²² in which the scaling function may be obtained within the cluster diffusion model.²³ The formula of universal scaling^{24,25} is

$$N_s \sim \theta s_{av}^{-2} f(s/s_{av}), \quad (9)$$

where N_s is the density of islands of size s , θ is the coverage, s_{av} is the average island size, and f is a scaling function that satisfies the relation

$$\int_0^\infty f(u) du = \int_0^\infty u f(u) du. \quad (10)$$

When applying the above scaling to results of our mean-field approximation we obtain the plots presented in Fig. 4. The universal scaling approach says nothing about the shape of scaling function. Only the equality given by Eq. (10) is required, but the shape of the scaling function proper depends on the details of the growth mechanism.

In Figs. 4(a) and 4(b) we present the computed original and scaled island size distributions. The shapes of the scaling functions are slightly different in the individual cases, but the

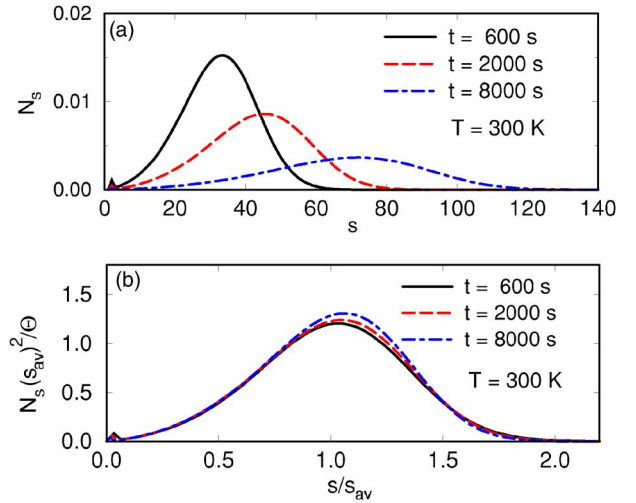


FIG. 6. (Color online) Scaling procedure for cluster size distributions at different time instants. The diagrams (a) and (b) show nonscaled and scaled distributions, respectively.

integrals of Eq. (10) overlap with less than a 5% error. The maxima of the scaling functions computed here are at $s/s_{av} \approx 1$, while those obtained in experiment and using KMC (Ref. 16) are placed distinctly at $s/s_{av} < 1$. The reason for this discrepancy is that our mean-field approximation does not include the cluster diffusion that produces the characteristic shape of the scaling function found by Kandel.²³

A similar scaling is applied to the island growth at different temperatures. The results are presented in Fig. 5; the maxima here correspond to $s/s_{av} \approx 1$ as well.

The general scaling procedure appears to be most accurate when applied to the evolution of cluster size distribution within the time range of the Ostwald ripening. This is easily seen from Figs. 6 and 3(b) where the scaling functions overlap.

IV. CONCLUSIONS

In this paper we describe the Pb mediated growth of Ge islands on Si(111) in a mean-field approximation, and we compare these results with experiment and with KMC simulations.¹⁷ The mean-field approach considerably simplifies the model calculation in comparison to the KMC method, and leads to a better understanding of the growth mechanism. In particular, we find that the threshold effect is clearly seen here, and we conclude that this is due to the chosen form of dissociation energy (1).

Another consequence of applying the formula (1) is that clusters tend to be compact, and that in their compact form they have enhanced stability. Comparison of the cluster size distributions obtained in this paper and in the KMC simulations shows that a pronounced cluster diffusion above the surfactant is expected. This phenomenon explains the observed unusual features of the Ge/Pb/Si(111).

- *Corresponding author. Electronic address: beben@ifd.uni.wroc.pl
- ¹M. Copel, M. C. Reuter, E. Kaxiras, and R. M. Tromp, Phys. Rev. Lett. **63**, 632 (1989).
- ²W. F. Egelhoff, Jr. and D. A. Steigerwald, J. Vac. Sci. Technol. A **7**, 2167 (1989).
- ³R. M. Tromp and M. C. Reuter, Phys. Rev. Lett. **68**, 954 (1992).
- ⁴H. Hibino, N. Shimizu, K. Sunitomo, Y. Shinoda, T. Nishioka, and T. Okano, J. Vac. Sci. Technol. A **12**, 23 (1994).
- ⁵M. Katayama, T. Nakayama, M. Aono, and C. F. McConville, Phys. Rev. B **54**, 8600 (1996).
- ⁶B. G. Liu, J. Wu, E. G. Wang, and Z. Zhang, Phys. Rev. Lett. **83**, 1195 (1999).
- ⁷J. Wu, B. G. Liu, Z. Zhang, and E. G. Wang, Phys. Rev. B **61**, 13212 (2000).
- ⁸V. Cherepanov, S. Filimonov, J. Myslivecek, and B. Voigtlander, Phys. Rev. B **70**, 085401 (2004).
- ⁹A. Portavoce, M. Kammler, R. Hull, M. C. Reuter, M. Copel, and F. M. Ross, Phys. Rev. B **70**, 195306 (2004).
- ¹⁰D. M. Wang, X. Sun, and Z. Q. Wu, Chin. Phys. Lett. **19**, 720 (2002).
- ¹¹D. M. Wang, X. Sun, Z. J. Ding, and Z. Q. Wu, Chin. Phys. Lett. **21**, 2029 (2004).
- ¹²D. Wang, Z. Ding, and X. Sun, Phys. Rev. B **72**, 115419 (2005).
- ¹³I.-S. Hwang, T.-C. Chang, and T. T. Tsong, Phys. Rev. Lett. **80**, 4229 (1998).
- ¹⁴T.-C. Chang, I.-S. Hwang, and T. T. Tsong, Phys. Rev. Lett. **83**, 1191 (1999).
- ¹⁵I.-S. Hwang, T.-C. Chang, and T. T. Tsong, Jpn. J. Appl. Phys., Part 1 **39**, 4100 (2000).
- ¹⁶J. Bęben, I.-S. Hwang, T.-C. Chang, and T. T. Tsong, Phys. Rev. B **63**, 033304 (2001).
- ¹⁷J. Bęben, I.-S. Hwang, and T. T. Tsong, Phys. Rev. B **64**, 235328 (2001).
- ¹⁸J. Bęben, I.-S. Hwang, and T. T. Tsong, Surf. Sci. **507**, 281 (2002).
- ¹⁹T. T. Tsong and R. Casanova, Phys. Rev. B **24**, 3063 (1981); Phys. Rev. Lett. **47**, 113 (1981).
- ²⁰W. H. Press, S. A. Teukolsky, W. T. Vetterling, and B. P. F. Flannery, *Numerical Recipes in Fortran* (Cambridge University Press, Cambridge, England, 1992).
- ²¹I. M. Lifshitz and V. V. Slyozov, J. Phys. Chem. Solids **19**, 35 (1961).
- ²²J. Li, A. G. Rojo, and L. M. Sander, Phys. Rev. Lett. **78**, 1747 (1997).
- ²³D. Kandel, Phys. Rev. Lett. **79**, 4238 (1997).
- ²⁴M. C. Bartelt and J. W. Evans, Phys. Rev. B **46**, 12675 (1992).
- ²⁵J. G. Amar, F. Family, and P.-M. Lam, Phys. Rev. B **50**, 8781 (1994).